Nanostructured Thin-Film Materials with Surface-Enhanced Optical Properties

Dustin J. Maxwell, Steven R. Emory, and Shuming Nie*

Department of Chemistry, Indiana University, Bloomington, Indiana 47405

Received November 16, 2000. Revised Manuscript Received January 22, 2001

We report the rational design and development of nanostructured thin-film materials that are highly efficient for surface-enhanced optical processes such as surface-enhanced Raman scattering (SERS). These materials consist of fractionated colloidal Ag particles in the size ranges of 30−50, 50−80, 80−100, and >100 nm. The basic rationale comes from correlated optical and topographic studies of single nanoparticles, which reveal a strong relationship between particle size and the excitation wavelength for efficient optical enhancement. The enhancement efficiencies are dependent on the particle size, the excitation wavelength, and the presence of activating ions such as Cl^- and Br^-. These nanostructured films provide a reproducible SERS substrate for ultrasensitive detection and spectroscopy of native biological molecules.

Introduction

Metal and semiconductor particles on the nanometer scale have unique optical, electronic, and magnetic properties that are not available in either isolated molecules or bulk solids.[1−8] These properties are currently under intense study for potential use in microelectronics, quantum dot lasers, nanoscale chemical sensors, data storage, and a host of other applications. Recent advances have led to large-scale preparation of highly monodisperse nanoparticles,[9−11] characterization of their lattice structures,[3−5] and fabrication of nanoparticle arrays[12−15] and light-emitting diodes.[16,17] For particles that are smaller than the exciton Bohr radius, a dominant effect is quantum-size confinement, which leads to the observation of discrete and narrow electronic states. Beyond this quantum-confinement regime (often in the size range of 10−100 nm), nanoparticles can also display optical or electronic properties that are dependent on size and shape. An example is the presence of a strong absorption band in the UV−vis spectra of metal nanoparticles such as silver, copper, and gold.[1,18,19] This absorption arises from collective free-electron oscillations (surface plasmon), and the resonance frequencies are strongly modulated by particle size, shape, and the surrounding medium.

Certain metallic nanoparticles also exhibit a phenomenon known as surface-enhanced Raman scattering (SERS) in which the scattering cross sections are dramatically enhanced for molecules adsorbed at appropriately roughened surfaces.[20,21] Since its discovery in 1977,[22,23] more than 3000 papers have been published dealing with fundamental mechanistic studies of photon−molecule−surface interactions as well as applications in electrochemistry, surface science, materials research, and biology.[20,21] While the fundamental mechanisms are still incompletely understood, it is believed that two simultaneously operative mechanisms, a long-range classical electromagnetic (EM) effect and a short-range "chemical" effect, are responsible for SERS.

* To whom correspondence should be addressed. E-mail: nie@indiana.edu.

(1) Halperin, W. P. *Rev. Mod. Phys.* **1986**, *58*, 533−606.
(2) Alivisatos, A. P. *Science* **1996**, *271*, 933−937; *J. Phys. Chem.* **1996**, *100*, 13226−13239.
(3) Brus, L. E. *Appl. Phys. A* **1991**, *53*, 465−474.
(4) (a) Henglein, A. *Chem. Rev.* **1989**, *89*, 1861−1873. (b) Schmid, G. *Chem. Rev.* **1992**, *92*, 1709−1727. (c) Hagfeldt, A.; Gratzel, M. *Chem. Rev.* **1995**, *95*, 49−68.
(5) Weller, H. *Angew. Chem., Int. Ed. Engl.* **1993**, *32*, 41−53.
(6) Fendler, J. H.; Meldrum, F. C. *Avd. Mater.* **1995**, *7*, 607−632.
(7) Wang, Y.; Herron, N. *J. Phys. Chem.* **1991**, *95*, 525−532.
(8) Gehr, R. J.; Boyd, R. W. *Chem. Mater.* **1996**, *8*, 1807−1819.
(9) Murray, C. B.; Norris, D. J.; Bawendi, M. G. *J. Am. Chem. Soc.* **1993**, *115*, 8706−8715.
(10) Bowen Katari, J. E.; Colvin, V. L.; Alivisatos, A. P. *J. Phys. Chem.* **1994**, *98*, 4109−4117.
(11) Hines, M. A.; Guyot-Sionnest, P. *J. Phys. Chem.* **1996**, *100*, 468−471.
(12) Murray, C. B.; Kagan, C. R.; Bawendi, M. G. *Science* **1995**, *270*, 1335−1338.
(13) Andres, R. P.; Bielefeld, J. B.; Henderson, J. I.; Janes, D. B.; Kolagunta, V. R.; Kubiak, C. P.; Mahoney, W. J.; Osifchin, R. G. *Science* **1996**, *273*, 1690−1693.
(14) (a) Heath, J. R.; Williams, R. S.; Shiang, J. J.; Wind, S. J.; Chu, J.; D'Emic, C.; Chen, W.; Stanis, C. L.; Bucchignano, J. J. *J. Phys. Chem.* **1996**, *100*, 3144−3149. (b) Harfenist, S. A.; Wang, Z. L.; Alvarez, M. M.; Vezmar, I.; Whetten, R. L. *J. Phys. Chem.* **1996**, *100*, 13904−13910.
(15) (a) Mirkin, C. A.; Letsinger, R. L.; Mucic, R. C.; Storhoff, J. J. *Nature* **1996**, *382*, 607−609. (b) Alivisatos, A. P.; Johnsson, K. P.; Peng, X.; Wilson, T. E.; Loweth, C. J.; Bruchez, M. P., Jr.; Schultz, P. G. *Nature* **1996**, *382*, 609−611.
(16) Colvin, V. L.; Schlamp, M. C.; Alivisatos, A. P. *Nature* **1994**, *370*, 354−356.
(17) Dabbousi, B. O.; Bawendi, M. G.; Onotsuka, O.; Rubner, M. F. *Appl. Phys. Lett.* **1995**, *66*, 1316−1318.
(18) Barber, P. W.; Chang, R. K. *Optical Effects Associated with Small Particles*; World Scientific: Singapore, 1988.
(19) Doremus, R. H. *J. Chem. Phys.* **1964**, *40*, 2389−2396.
(20) (a) *Surface-Enhanced Raman Scattering*; Chang, R. K., Furtak, T. E., Eds.; Plenum Press: New York, 1981. (b) Moskovits, M. *Rev. Mod. Phys.* **1985**, *47*, 783−826. (c) Campion, A.; Kambhampati, P. *Chem. Soc. Rev.* **1998**, *27*, 241−250.
(21) *Fundamentals and Applications of Surface Raman Spectroscopy*; Garrell, R. L., Pemberton, J. E., Eds.; VCH Publishers: Deerfield Beach, FL, 1994.
(22) Jeanmaire, D. L.; Van Duyne, R. P. *J. Electroanal. Chem.* **1977**, *84*, 1−20.
(23) Albrecht, M. G.; Creighton, A. J. *J. Am. Chem. Soc.* **1977**, *99*, 5215−5217.

10.1021/cm0009120 CCC: $20.00
Published on Web 02/28/2001

Recent research by several groups has examined the intrinsic surface-enhanced Raman properties of single Ag and Au nanoparticles.[24−29] The results indicate that a very small fraction of colloidal nanoparticles is highly efficient for optical enhancement, yielding enormous enhancement factors on the order of $10^{14}-10^{15}$. This discovery has opened new possibilities for developing novel nanostructured materials. In particular, correlated SERS and topographic studies of single Ag nanoparticles have revealed a strong relationship between the particle size and the excitation wavelength.[24] For example, 90-nm Ag particles are most efficiently excited at 514 nm, while 140-nm Ag particles are best excited at 570 nm. For efficient excitation at 647 nm, it is necessary to form nanoparticle aggregates as large as 190−200 nm in diameter. In comparison, the SERS-active gold particles at 647-nm excitation are small nanocrystals in the size range of 63 ± 3 nm. Thus, by sorting colloidal particles into different size fractions, it should be possible to rationally design nanostructured materials with enhanced optical properties.

In this paper, we report the rational design and development of nanostructured thin films by using size-fractionated colloidal nanoparticles. These thin films have a shiny, metallic appearance because of electronic coupling among the constituent particles, but they also retain some of the key characteristics associated with single particles such as size-dependent optical enhancement and activation by chloride ions. We show that the nanostructured films provide a new type of substrate materials for developing SERS as an ultrasensitive analytical tool.

Experimental Section

Reagents. All chemicals and materials were used as received: adenine (Aldrich), amoxicillin (Sigma), 1,2-bis(4′-pyridyl)ethylene (Aldrich), crystal violet (Fisher Scientific), polylysine hydrobromide (Sigma), rhodamine 6G perchlorate (Aldrich), silver nitrate (99+%, Aldrich), and sodium chloride (99.8% Mallinckrodt). Stock solutions of adenine, amoxicillin, 1,2-bis-(4′-pyridl)ethylene, crystal violet, and rhodamine 6G were prepared in spectrophotometric-grade methanol (99.9% Aldrich) before being diluted in water to the required concentrations. Ultrapure water (18 $m\Omega^{-1}$, Millipore, Bedford, MA) was used throughout the experiment.

Colloid Fractionation and Thin-Film Preparation. Silver colloids were prepared by the citrate-reduction procedure of Lee and Miesel.[30] Sodium citrate (5 mL of a 1% solution) was added to a boiling flask of ultrapure water (250 mL) containing silver nitrate (45 mg) and continued to boil for 1 h. Morphological examination by transmission electron microscopy (TEM) revealed that the colloids were a heterogeneous mixture of particles with an average particle size of 35−50 nm. The colloidal particles were then separated through a sequential filtration process, using a series of polycarbonate membranes (Osmonics, Livermore, CA) with 100-, 80-, 50-, and 30-nm pore sizes (Figure 1). These track-etched membranes have relatively uniform and straight pores (∼5% standard deviation) and have been used as templates in nanomaterials synthesis.[31] After each filtration step, the particles retained on the film surface were collected and resuspended in 0.1% (w/w) sodium citrate solution. The first fraction contained particles >100 nm in diameter, the second fraction between 80 and 100 nm, the third fraction between 50 and 80 nm, and the fourth fraction between 30 and 50 nm. The concentration of colloidal particles in each fraction was estimated by both UV−vis absorption (note: the molar extinction coefficient is dependent on the particle size) and by direct AFM imaging of the immobilized particles. Because a known volume of a colloid solution was used in the immobilization experiment, the colloid concentration could be calculated from the total number of particles detected by AFM.

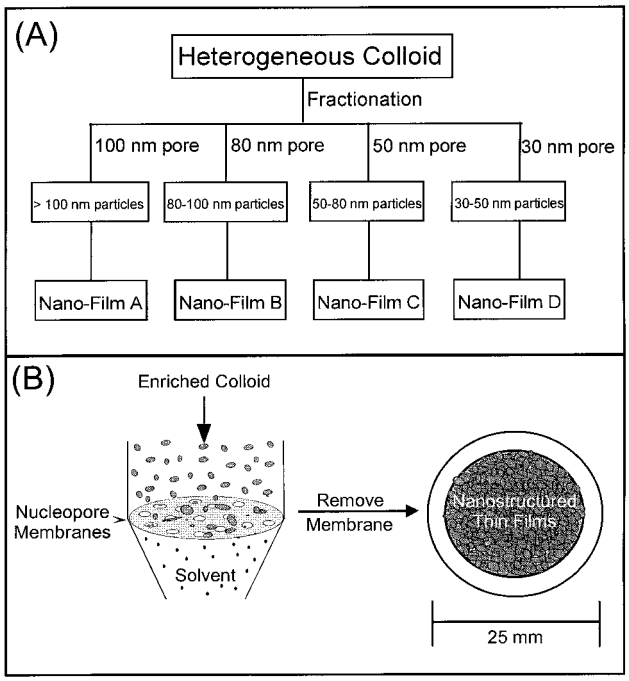

Figure 1. Schematic diagrams showing (A) colloid fractionation by sequential filtration with 100-, 80-, 50-, and 30-nm pore membranes and (B) preparation of thin-films nanomaterials by filtering fractionated colloids on a membrane with pores smaller than the particles. See text for detailed explanation.

To prepare nanostructured thin films, each fraction was filtered through a membrane with a pore size smaller than the particle diameter. After all the solvent was filtered through, the membrane was removed and dried at room temperature for 30 min. This process yielded a shiny metallic-looking film containing immobilized nanoparticles with a narrow size distribution (about 20−30-nm size spread) (Figure 1B). The density of immobilized particles was controlled by the volume and concentration of the fractionated colloids. Assuming uniform particle distribution, the surface coverage was estimated by calculating the total number of particles and the area occupied by each particle.

Instrumentation. A confocal microscope was constructed using a Nikon Diaphot 200 inverted microscope and a continuous-wave argon ion laser (Lexel Laser, Fremont, CA). This

(24) (a) Nie, S.; Emory, S. R. *Science* **1997**, *275*, 1102−1106. (b) Emory, S. R.; Haskins, W. E.; Nie, S. *J. Am. Chem. Soc.* **1998**, *120*, 8009−8010. (c) Emory, S. R.; Nie, S. *J. Phys. Chem. B* **1998**, *102*, 493−497. (d) Krug, J. T., II.; Wang, J. D.; Emory, S. R.; Nie, S. *J. Am. Chem. Soc.* **1999**, *121*, 9208−9214.

(25) (a) Kneipp, K.; Wang, Y.; Kneipp, H.; Perelman, L. T.; Itzkan, I.; Dasari, R. R.; Feld, M. S. *Phys. Rev. Lett.* **1997**, *78*, 1667−1670. (b) Kneipp, K.; Wang, Y.; Kneipp, H.; Itzkan, I.; Dasari, R. R.; Feld, M. S. *Phys. Rev. Lett.* **1996**, *76*, 2444−2447. (c) Kneipp, K.; Kneipp, H.; Itzkan, I.; Dasari, R. R.; Feld, M. S. *Chem. Rev.* **1999**, *99*, 2957−2976.

(26) Michaels, A. M.; Nirmal, M.; Brus, L. E. *J. Am. Chem. Soc.* **1999**, *121*, 9932−9939.

(27) (a) Xu, H.; Bjerneld, E. J.; Käll, M.; Borjesson, L. *Phys. Rev. Lett.* **1999**, *83*, 4357−4360. (b) Xu, H.; Aizpurua, J.; Käll, M.; Apell, P. *Phys. Rev. E* **2000**, *62*, 4318−4324.

(28) Moyer, P. J.; Schmidt, J.; Eng, L. M.; Meixner, A. J. *J. Am. Chem. Soc.* **2000**, *122*, 5409−5410.

(29) Haslett, T. L.; Tay, L.; Moskovits, M. *J. Chem. Phys.* **2000**, *113*, 1641−1646.

(30) Lee, P. C.; Meisel, D. *J. Phys. Chem.* **1982**, *86*, 3391−3395.

(31) Martin, C. R. *Science* **1994**, *266*, 1961−1966; *Acc. Chem. Res.* **1995**, *28*, 61−68.

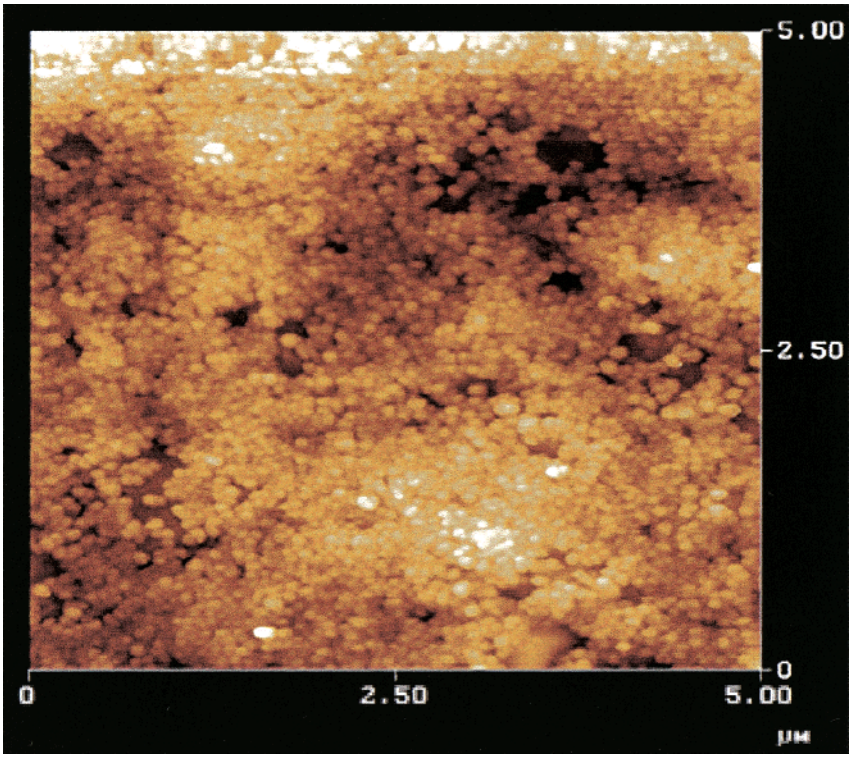

Figure 2. Tapping-mode AFM image of a nanostructured thin film prepared from 50- to 80-nm Ag colloidal particles. Note the presence of distinct nanoparticles in an uneven distribution.

microscope system contained the following: (1) a Nikon 40× microscope objective to collect the backscattered Raman photons; (2) a single stage, high throughput spectrograph (Model 270M, Spex, Edison, NJ) with an aspheric focusing lens (f = 1.85, NA = 0.15, Thorlabs, Newton, NJ); (3) a thermoelectrically cooled, back-illuminated CCD camera (Princeton Instruments, Trenton, NJ). A video-rate-intensified CCD camera (Photon Technology International, South Brunswick, NJ) was mounted on the front port of the microscope for wide-field imaging.

A compact Raman instrument, Solution 633 (Detection Limit, Laramie, WY) was used to examine samples at 633 nm.[32] This instrument utilized a fiber-optic probe that connected a fiber-optic cable to a 40-mW HeNe laser and an F/2 spectrograph. A thermoelectrically cooled CCD camera (Kodak 0400 CCD) was coupled to the spectrograph. *DLSPEC* software (Detection Limit) was used for both data acquisition and spectral processing.

Results and Discussion

Film Morphology and Optical Properties. A striking feature of the nanostructured thin films is their shiny and metallic appearance (Figure 2A). To investigate whether the constituent nanoparticles are still distinct or have coalesced into bulk metal, we have used tapping-mode atomic force microscopy (AFM) to examine the film morphology on a nanometer scale (Figure 2B). The result shows distinct nanoparticles and nanoaggregates, with an uneven distribution on the membrane surface. Examination with transmission electron microscopy reveals that the particles tend to assemble around the pores and form aggregates as more particles are deposited. Thus, the metallic color arises from strong electronic coupling among the particles, not from particle coalescence. Natan and co-workers reported a similar effect for Au particle multilayers prepared with a short molecular linker.[33] In the present work, negatively charged citrate ions (used for colloid stabilization) are present on the particle surface, and the nanostructured thin films are prepared without specific linker molecules.

Figure 3 compares the SERS signal intensities of rhodamine 6G obtained from a nanostructured thin film and from colloidal nanoparticles immobilized on glass surfaces. In the latter case, glass cover slips were coated with mercaptopropyl trimethoxysilane (mercapto groups bind to Ag particles through a sulfur−metal bond)[34,35] or with polylysine (positively charged amine groups bind to negatively charged particles by electrostatic interactions).[24] AFM studies revealed that the majority of the immobilized particles were isolated single particles at low colloid concentrations ($<10^{-11}$ M). As shown in Figure 3, the nanostructured thin films are highly efficient for surface Raman enhancement, and the SERS signal intensities are 5−10 times higher than those obtained with alternative methods.

Several factors appear to be responsible for the observed increase in the SERS intensities. First, our procedure does not require chemical modification, and thus the particle surface is more readily available for analyte adsorption. Molecular linkers containing thiols

(32) Mullen, K.; Carron, K. T. *Anal. Chem*. **1994**, *66*, 478.

(33) (a) Musick, M. D.; Keating, C. D.; Keefe, M. H.; Natan, M. J. *Chem. Mater*. **1997**, *9*, 1499−1501. (b) Brown, K. R.; Lyon, L. A.; Fox, A. P.; Reiss, B. D.; Natan, M. J. C*hem. Mater*. **2000**, *12*, 314−323.

(34) (a) Chumanov, G.; Sokolov, K.; Gregory, B. W.; Cotton, T. M. *J. Phys. Chem*. **1995**, *99*, 9466−9471. (b) Fritzsche, W.; Symanzik, J.; Sokolov, K.; Cotton, T. M.; Henderson, E. *J. Colloid Interface Sci*. **1997**, *185*, 466−472.

(35) (a) Freeman, R. G.; Grabar, K. G.; Allison, K. A.; Bright, R. M.; Davis, J. A.; Guthrie, A. P.; Hommer, M. B.; Jackson, M. A.; Smith, P. C.; Walter, D. G.; Natan, M. J. *Science* **1995**, *267*, 1629−1632. (b) Grabar, K. G.; Brown, K. R.; Keating, C. D.; Stranick, S. J.; Tang, S.-L.; Natan, M. J. *Anal. Chem*. **1997**, *69*, 471−477. (c) Grabar, K. C.; Freeman, R. G.; Hommer, M. B.; Natan, M. J. *Anal. Chem*. **1995**, *67*, 735−743.

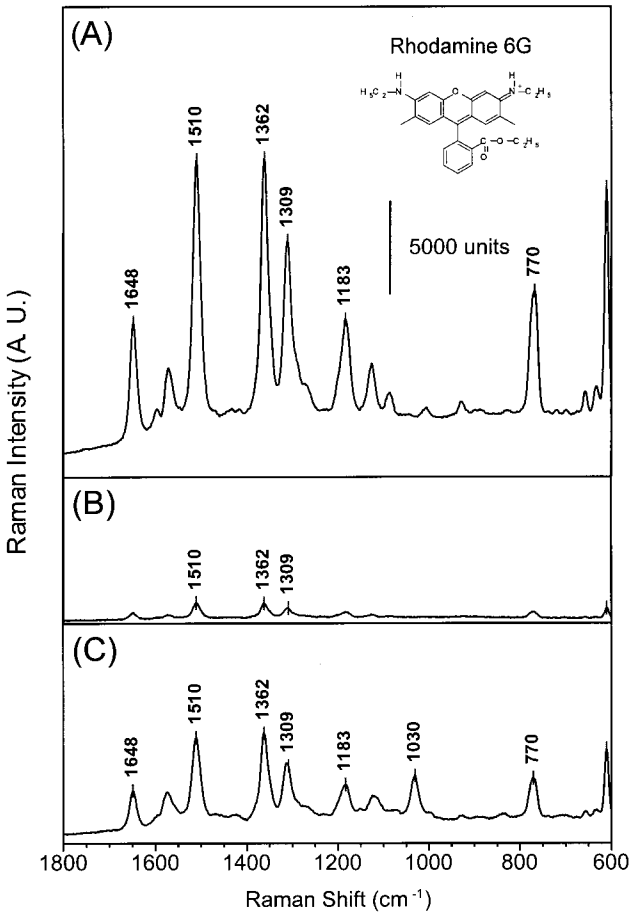

Figure 3. Comparison of SERS intensities between nanostructured thin films and colloidal nanoparticles immobilized on chemically modified surfaces. (A) Film prepared from fractionated Ag colloids (>100-nm fraction); (B) unfractionated colloids immobilized on a glass slide surface by using mercaptopropyl trimetroxysilane; and (C) unfractionated colloids immobilized on a glass surface by using polylysine. Laser wavelength = 633 nm; excitation intensity = 3 mW; data integration time = 1 s; and R6G concentration = 1×10^{-7} M.

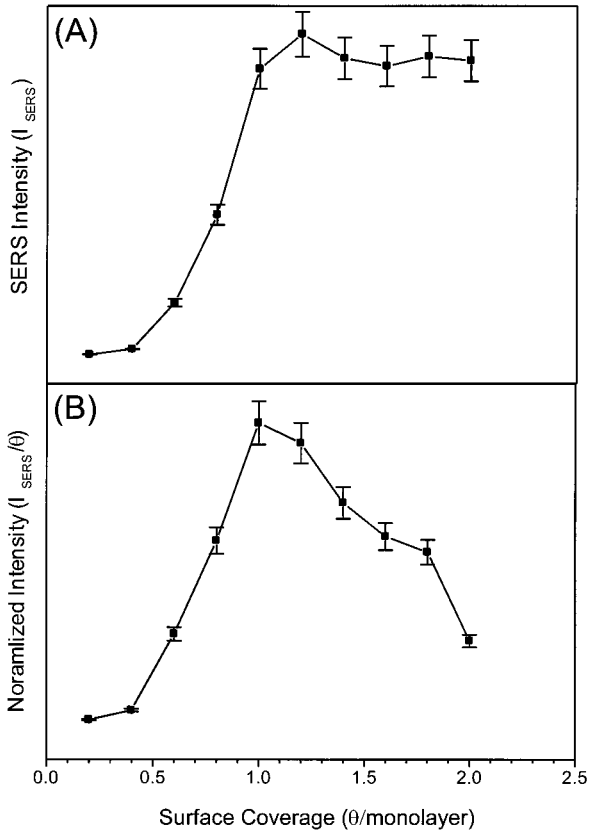

Figure 4. (A) Plot of the SERS signal intensities as a function of particle coverage (θ) and (B) plot of the normalized SERS intensities (I_{SERS} divided by θ) vs particle coverage. I_{SERS} is the average value of 10 measurements of the peak height at 1640 cm^{-1} (a characteristic Raman line of BPE). Error bars represent intensity variations at 2 standard deviations.

can "spoil" the surface or block adsorption. Also, the physical filtration procedure allows more particles to be deposited on a surface than the thiol or polylysine method that rely on passive electrostatic or chemical adsorption of the nanoparticles. Interparticle forces such as electrostatic repulsion tend to reduce the particle packing density. Better surface adsorption and higher particle densities should both lead to increased SERS intensities per unit area. Second, the filtration process selects colloidal particles in a particular size range, which effectively concentrates the particles that are SERS-active at specific excitation wavelengths. Third, electronic coupling among the constituent particles is expected to increase the enhancement efficiencies, a phenomenon commonly observed in electrolyte-induced colloid aggregation.

Effect of Particle-to-Particle Coupling. As mentioned above, the film's metallic appearance indicates electronic coupling among the particles. It is thus important to investigate how this coupling effect might change the optical enhancement properties of Ag nanoparticles. Figure 4 shows both the observed and surface-coverage-normalized SERS intensities as a function of the particle coverage (θ) on the membrane surface. The particle density was calculated by the volume and concentration of the fractionated colloids. The surface coverage was estimated by using the total number of particles and the area occupied by each particle. For each coverage value, 10 measurements were made using BPE as the probe molecule. The SERS intensity was the average value of the Raman peak height at 1636 cm^{-1}. The surface coverage was confirmed by direct AFM imaging.

In the absence of particle−particle interactions, one would expect a linear relationship between the SERS intensity and the surface coverage and a constant line for the normalized SERS intensity. Deviations from these relationships would indicate electronic coupling among the particles. Indeed, the SERS intensity increases rapidly from ≈0.5 monolayer to 1.0 monolayer particle coverage. The data in Figure 4 show three distinct regions: (a) From 0 to 0.5 monolayer coverage, the SERS intensity increases slowly with the number of particles. The relation is approximately linear because the particle−particle coupling is weak at these surface coverage levels. (b) From 0.5 to 1.0 monolayer coverage, the SERS intensity increases in a nonlinear fashion because the constituent particles start to couple with each other. (c) Beyond one monolayer, the absolute intensity reaches a plateau. This leveling-off behavior suggests that the thin films behave as a two-dimensional surface instead of as a three-dimensional object. The reasons are likely related to light scattering, surface accessibility, and surface plasmon resonance changes as the film thickness increases.

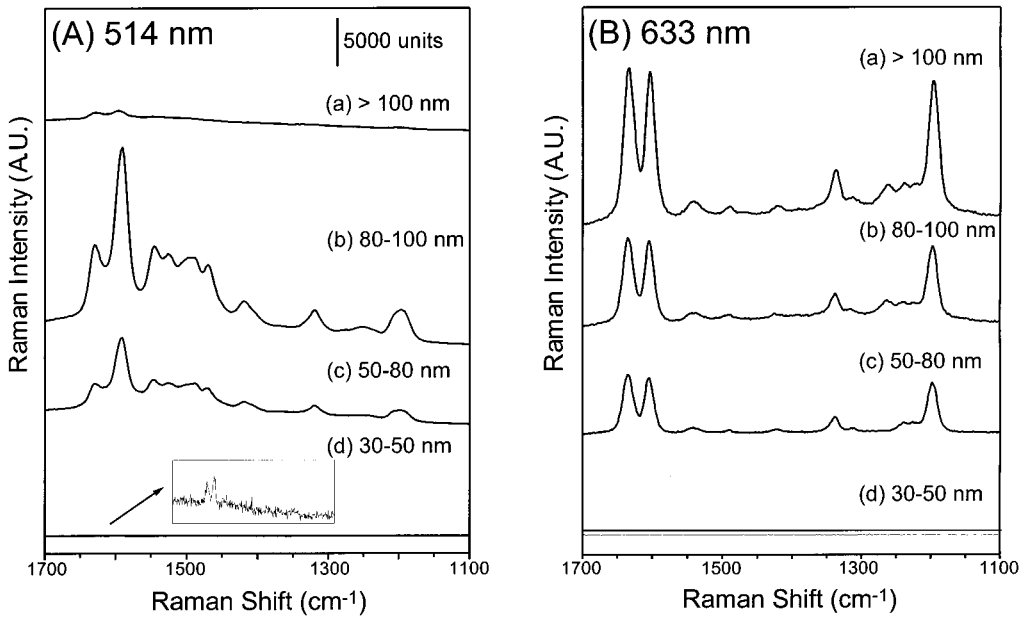

Figure 5. SERS spectra of BPE obtained from four nanostructured films containing Ag particles in the following size ranges: (a) >100 nm, (b) 80−100 nm, (c) 50−80 nm, and (d) 30−50 nm. Two sets of spectra were obtained at 514- and 633-nm laser excitation. BPE concentration = 1 μM; integration time = 1 s; laser power = 1 μW at 514 nm, and 3 mW at 633 nm.

To determine whether the nanostructured films retain the size-tunable optical properties of individual particles, a set of four thin films were prepared using the fractionated colloids, and SERS spectra were obtained at both 514- and 633-nm excitation wavelengths (Figure 5). The spectra at these two wavelengths are significantly different in relative peak intensities because the adsorbed BPE molecules tend to dimerize at 514-nm excitation (but not at 633 nm).[36] It should also be noted that BPE itself does not have electronic transitions in the visible, and conventional resonance enhancement should thus be minimal at both 514 and 633 nm. As shown in Figure 5, the intensities of SERS signals from the nanostructured films of nearly identical thickness (about 1 monolayer) are strongly dependent on the particle size and the excitation wavelength. The film containing 80−100-nm particles exhibits the highest enhancement efficiency at 514-nm excitation, while the film with >100-nm particles is most efficient at 633-nm excitation. With colloidal particles smaller than 50 nm, no SERS signals or only extremely weak signals could be detected. This result is similar to the size-dependent enhancement behavior reported for single Ag particles.[24] Considering the extent of particle−particle coupling, it is surprising that the nanostructured films still retain some of the size-tunable characteristics associated with isolated particles. Further support for this conclusion comes from micro-Raman imaging, which reveals the presence of single blinking particles in the film.[37] This result demonstrates the rational design of nanostructured materials that are tuned to specific excitation wavelengths for surface optical enhancement.

Chloride Ion Activation. Previous work by Hildebrandt and Stockburger[38] suggests that the SERS-active sites are high-affinity binding sites (65 kJ/mol) associated with adsorbed anions such as chloride or bromide. The number of active sites per colloidal silver particle is very small (about 3.3 on average), which leads to a rapid saturation of the SERS intensities with increasing analyte concentration. Single-particle as well as bulk studies also indicate that chloride ions can activate and aggregate colloidal nanoparticles.[24] It is important to investigate how the presence of chloride ions might influence the optical enhancement properties of the nanostructured films. Because all the particles are firmly immobilized on the membrane surface, any chloride effect would primarily come from surface activation. To rule out the possibility of aggregation, transmission electron microscopy (TEM) was used to examine the nanoscale morphology of the nanostructured films before and after treatment with 1.0 M sodium chloride. The result confirmed that chloride ions did not induce particle aggregation on the nanometer scale.

Figure 6 shows the SERS spectra of BPE obtained from a thin film in the absence and presence of 20 mM NaCl. Clearly, the presence of chloride ions has an activation effect that leads to a 2-fold increase in the SERS signal intensities and a 1.5-fold decrease in the background level. The combined outcome is a significant improvement in the signal-to-noise ratios. These population-averaged results are similar to, but less pronounced than, the activation effect observed for single particles.[4,24] We believe that the chloride ions are most likely associated with the SERS-active sites in the nanostructured film. There is considerable evidence in the literature indicating that surface-active sites play an important role in SERS.[39] These sites are believed

(36) (a) Van Duyne, R. P.; Hulteen, J. C.; Treichel, D. A. *J. Chem. Phys.* **1993**, *99*, 2101−2115. (b) Hulteen, J. C.; Treichel, D. A.; Smith, M. T.; Duval, M. L.; Jensen, T. R.; Van Duyne, R. P. *J. Phys. Chem. B.* **1999**, *103*, 3854−3863.

(37) Maxwell, D. J.; Han, M.-Y.; Nie, S., unpublished results.

(38) Hildebrandt, P.; Stockburger, M. *J. Phys. Chem.* **1984**, *88*, 5935.

(39) Otto, A.; Mrozek, I.; Grabhorn, H.; Akemann, W. *J. Phys. Condens. Matt.* **1992**, *4*, 1143−1212.

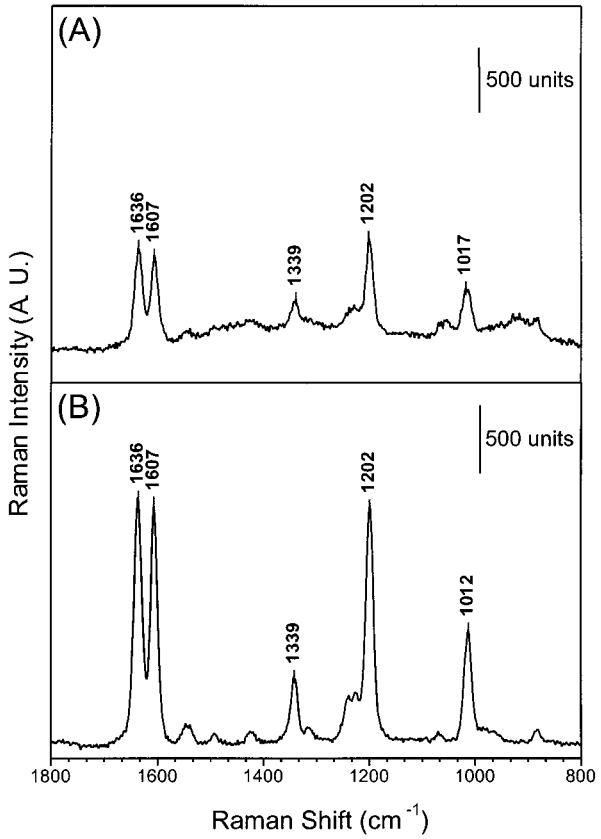

Figure 6. Surfaced-enhanced Raman scattering spectra of BPE obtained from a nanofilm (>100-nm particle sizes) (A) without sodium chloride and (B) with 20 mM sodium chloride. Laser wavelength = 633 nm; excitation intensity = 3 mW; data integration time = 1 s; and BPE concentration = 1 μM.

to be adatoms, atomic clusters, sharp steps, or edges. They are responsible for chemical enhancement via resonant charge-transfer and resonance Raman-like enhancement.[40] While the structure and properties of SERS-active sites are still unclear, this work demonstrates that ultrasensitive surface-enhanced Raman studies can benefit from the use of dilute chloride ions.

Applications. When activated with chloride ions, the nanostructured thin films are well suited for sensitive analysis and identification of underivatized samples in small volumes (nanoliter to microliter). Unlike fluorescence emission, Raman scattering is a vibrational spectroscopic technique that yields detailed fingerprint information at room temperature. In Figure 7 are shown representative SERS spectra obtained from three samples (BPE, R6G, and crystal violet) ranging in concentration from 10^{-8} to 10^{-9} M. The sample volumes were about 1 μL, spread over a 1.0-cm^2 area on the film. Considering the sampling area ($\sim$100 μm in diameter), the amount of analyte molecules being probed was about 1 attomole or $\sim 6.0 \times 10^5$ molecules. Using cyclohexane as a standard, we estimate that the enhancement factors achieved on the nanostructured films are in the range of 10^9–10^{10}. These values are smaller than that derived from single-molecule measurement,[24] but are substantially larger than those reported with other SERS-active materials.[21] The observed enhancement factors should

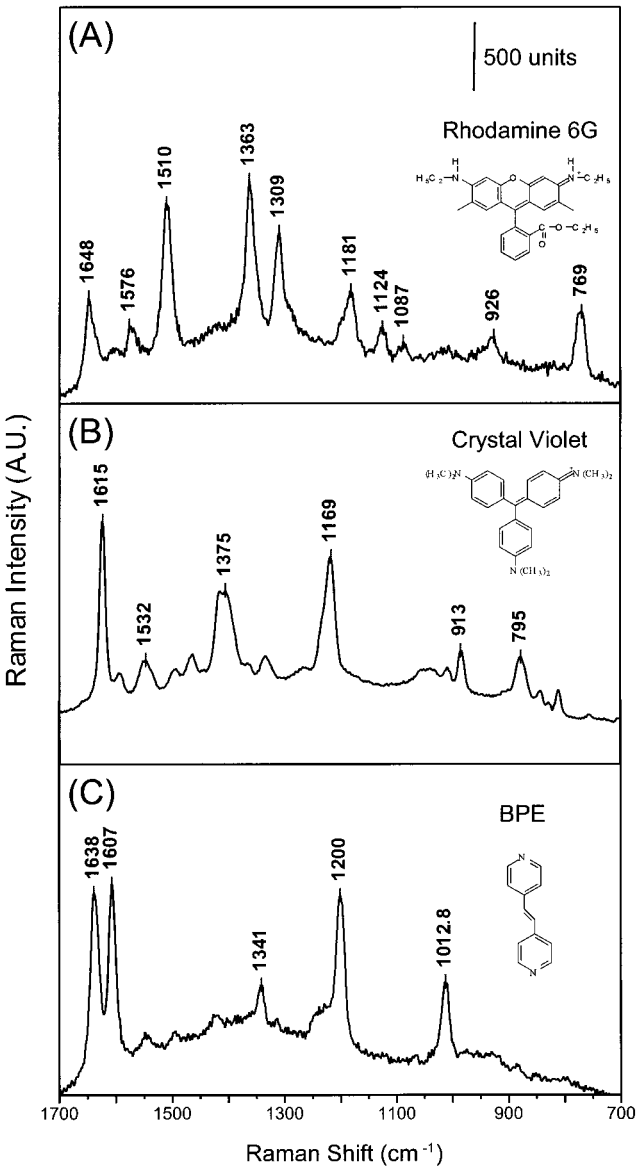

Figure 7. Surface-enhanced Raman spectra obtained from small-volume samples at low concentrations: (A) 1.0×10^{-9} M R6G; (B) 1.0×10^{-9} M crystal violet; and (C) and 1.0×10^{-8} M BPE. Sample volume = 1.0 μL; laser wavelength = 633 nm; excitation intensity = 3 mW; and data integration time = 1 s.

approach the single-molecule limit (that is, 10^{14}–10^{15}) at extremely low concentrations because most of the analyte molecules are expected to migrate and adsorb at SERS-active sites.[38] Furthermore, the SERS spectrum was found to be highly reproducible, with a standard deviation of 5–10% from region to region on the film.

To further explore the use of nanostructured films to detect biomolecules, we have examined the native DNA base adenine and the antibiotic drug amoxicillin (Figure 8). The SERS spectrum of adenine is in agreement with previous data,[41] with a characteristic Raman line at 732 cm^{-1}. Kneipp et al. have shown that single adenine molecules might be detected and identified by using SERS and that the ability to differentiate unlabeled

(40) (a) Lombardi, J. R.; Birke, R. L.; Tu, T.; Xu, J. *J. Chem. Phys.* **1986**, *84*, 4174. (b) Kambhampati, P.; Child, C. M.; Campion, A. *J. Chem. Soc., Faraday Trans.* **1996**, *92* (23), 4775.

(41) Kneipp, K.; Kneipp, H.; Kartha, V.; Manoharan, R.; Deineum, G.; Itzkan, I.; Dasari, R. R.; Feld, M. S. *Phys. Rev. E* **1998**, *57*, R6281–84.

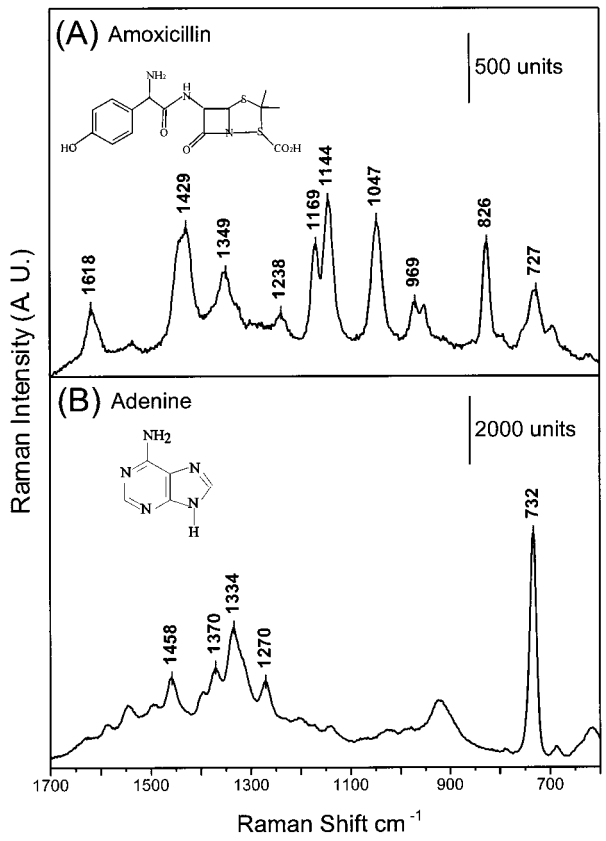

Figure 8. Surface-enhanced Raman spectra of native biological molecules adsorbed on nanostructured thin films (>100-nm particle sizes): (A) amoxicillin and (B) adenine. Laser wavelength = 633 nm; excitation intensity = 3 mW; data integration time = 1 s; amoxicillin concentration = 1 μM; and adenine concentration = 1 μM.

DNA bases is important to single-molecule DNA sequencing.[41] To our knowledge, the SERS spectrum of amoxicillin has not been reported previously. This antibiotic drug was chosen for SERS studies because a trace amount of this compound is usually found in milk and dairy products (due to its use in animal feed).[42] Human consumption of such milk may lead to the development of antibiotic resistance. It is thus important to determine the residual amount of amoxicillin in drinking milk samples. SERS appears to be an excellent tool for both identifying and quantifying this antibiotic compound. The spectrum in Figure 8 contains many spectral signatures that are useful for molecular identification. Although we have not quantitatively studied the relationship between the SERS signal intensity and antibiotic concentration, preliminary results indicate that reliable identification can be made from 10^{-6}–10^{-9} M, a concentration range that should be useful for whole milk studies.

In summary, we have developed nanostructured thin films that are highly efficient for surface-enhanced Raman scattering. By separating heterogeneous nanoparticles into different size fractions, we have prepared a set of four nanofilms and have studied their morphological and optical properties. The results reveal that the nanostructured films exhibit the key characteristics of single particles such as size-dependent optical enhancement and surface activation. This allows the rational design of nanostructured materials that are most efficiently excited for surface optical enhancement at specific wavelengths. Potential applications of such rationally designed materials include ultrasensitive optical detection and spectroscopy of native biological molecules such as DNA bases and antibiotic drugs.

Acknowledgment. This work was supported in part by grants from the Department of Energy (DOE FG02-98ER14873) and the National Science Foundation (CHE-9610254) for financial support. We are also grateful to John Krug, Kyle Kimble, and William Doering for technical help.

CM0009120

(42) (a) Sorensen, L. K.; Rasmussen, B. M.; Boison, J. O.; Keng, L. *J. Chromatogr. B: Biomed. Sci. Appl.* **1997**, *694*, 383–391. (b) Luo, W.; Hansen, E. B., Jr.; Ang, C. Y. W.; Deck, J.; Freeman, J. P.; Thompson, H. C. *J. Agric. Food Chem.* **1997**, *45*, 1264–1268. (c) Liang, P.; Sanchez, R. I.; Martin, M. T. *Anal. Chem.* **1996**, *68*, 2426–2431.